

Numerical Investigation on Power Outputs of a Wind Turbine Sited over Continuous Hilly Terrain

ZHOU Tianyi, TAN Jianfeng*, CAI Jiangang, SHI Ruipeng, XIA Yunsong

School of Mechanical and Power Engineering, Nanjing Tech University, Nanjing 211816, P.R. China

(Received 4 June 2019; revised 30 December 2019; accepted 19 January 2020)

Abstract: The location of wind turbines on a continuous hilly terrain has an influence on its power outputs. A CFD-based approach is developed to investigate the complex aerodynamic interference between two wind turbines and the hilly terrain. In this approach, a new three-dimensional model of hilly terrain is established to analyze its viscous effect, and a wind shear is modelled through logarithmic function. They are coupled into the aerodynamics of wind turbine based on “FLUENT” software. Then we apply the proposed method to the NREL Phase VI wind turbines and compare with an experiment in the atmospheric boundary layer (ABL) wind tunnel to validate its accuracy. The simulation also investigates the power outputs of wind turbines on the flat ground and the continuous hilly terrain by changing the location of the wind turbine related to the hilly terrain and the shape of the 1st hill. The results show that the wind turbine located on the top of the 2nd hill has the maximum power; and that when the wind turbine is located on the downstream of the hill, the stall zone should be avoided, and the power of the wind turbine located on the side of the hill is higher than that of the wind turbine located on the front and rear of the hilly terrain.

Key words: power characteristics; wind shear function; NREL wind turbine; continuous hilly terrain; simulation analysis

CLC number: O355

Document code: A

Article ID: 1005-1120(2020)01-0120-09

0 Introduction

Fossil energy has brought about a series of environmental problems, and renewable energy, like wind energy, is attracting researcher's attention. But its high level of requirement that wind turbines should output power as high as possible under limited conditions for normal operation and maintenance hinders its spread.

Several studies have investigated the power output of wind turbine affected by land hills. Wei et al.^[1-3] conducted a wind tunnel test, and found that the wind speed and wind turbine power output in front of a single hill composed of a two-dimensional Gaussian curve were reduced, and it was relative to the flat terrain, in the case of constant wind speed in the vertical direction. Porté-Agel et al.^[4] found that the output of the wind turbine at the top of a single mountain was significantly increased with

the acceleration effect of the flow field. Wei et al.^[5-7] used the wind tunnel experiment to investigate the influence of the hill on the flow field, and the results indicated that the blockage effect of a single hill on the flow field, including wind velocity, wind direction, and wind turbulence, was significant. Shu et al.^[8] found that the length, width of the hill and the distance between the wind turbines were important factors related to the interference effect. Song et al.^[9-11] argued that it was necessary to effectively arrange the locations of wind turbines in complex terrain, and the power generation of complex terrain wind farms was stronger than that in flat terrain wind farms. Richards et al.^[12] found, via the contrast of numerical investigations on some turbulence models, including the standard $k-\epsilon$, RNG $k-\epsilon$, Wilcox $k-\omega$, SST $k-\omega$ and LRR QI turbulence models, that the SST $k-\omega$ was suitable for simulating rotat-

*Corresponding author, E-mail address: jianfengtan@njtech.edu.cn.

How to cite this article: ZHOU Tianyi, TAN Jianfeng, CAI Jiangang, et al. Numerical investigation on power outputs of a wind turbine sited over continuous hilly terrain[J]. Transactions of Nanjing University of Aeronautics and Astronautics, 2020, 37(1):120-128.

<http://dx.doi.org/10.16356/j.1005-1120.2020.01.011>

ing flow fields. Ivanell et al. [13-14] found that the wake generated by the upstream wind turbine reduced the wind speed in the downstream area, and increased the wind turbulence, leading to the decrease of the wind energy density around and the efficiency of wind energy of the downstream wind turbine. Palma et al. [15-17] used computational fluid dynamics solver, FLUENT, to model and simulate complex terrain, and better realized the three-dimensional turbulence simulation of hilly airflow in low-level complex terrain. Most of these investigations were based on a constant wind speed field and a two-dimensional single mountain model. The effect of the natural wind speed, which has a gradient change, and the impact of power and aerodynamic characteristics resulted from the downhill terrain on the left and right slopes of the hill, have rarely been taken into account. Furthermore, those investigations were mainly focused on single terrain.

Therefore, there is a need for an aerodynamic method of wind turbine that considers the effect of natural wind and three-dimensional effect of the hill. This paper establishes a NREL wind turbine aerodynamic model based on computational fluid dynamics solver, FLUENT, and constructs a three-dimensional hilly terrain model and wind shear model to obtain aerodynamic characteristics of the wind turbines. The pressure and flow field of the NREL Phase VI wind turbine are predicted. We conduct an experiment in the atmospheric boundary layer (ABL) wind tunnel to validate the accuracy of the proposed aerodynamic analysis method. The influence of the three-dimensional hilly terrain on the aerodynamic characteristics of the wind turbines can help to locate better positions of the wind turbine over complex terrain.

1 Computational Method

1.1 Aerodynamic model of wind turbine

1.1.1 Wind turbine CATIA modeling

The width and length of the wind tunnel are 50 m, and the radius, hub height, tip pitch angle, rotational speed, rated power, and airfoil are 5.029 m, 12 m, 3° , 72 r/min, 20 kW, S809, re-

spectively. Detailed parameters of the wind turbine can be found in the NREL Phase VI wind turbine experimental report [18]. From the blade 0.25R to 1.0R, the airfoil curve is generated every 0.05R section, then all the sections are smoothly connected by the spline curve, and the multi-section surface is used for forming. Then the blade, the hub, the nacelle and the tower are assembled to obtain a complete three-dimensional model of the NREL Phase VI wind turbine as shown in Fig.1. The actual object for the NREL Phase VI wind turbine is shown in Fig.2.

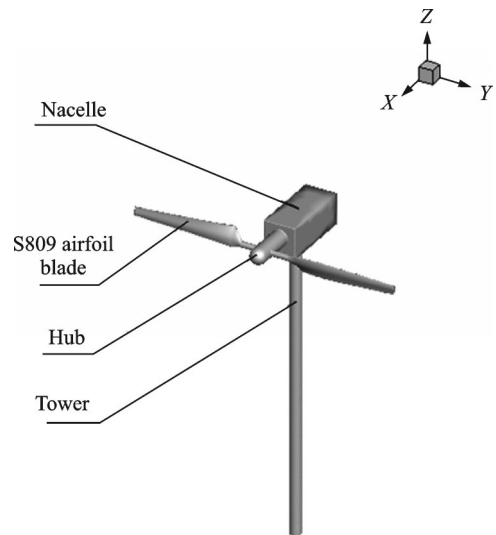


Fig.1 Wind turbine model

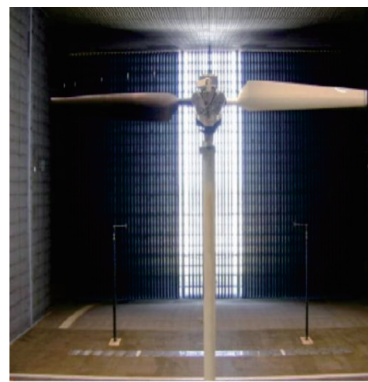


Fig.2 NREL Phase VI wind turbine in wind tunnel experiment

1.1.2 Boundary conditions for numerical calculation

The distribution of boundary conditions is shown in Fig.3. The velocity-inlet is used to model the boundary layer of inlet, and the UDF (User de-

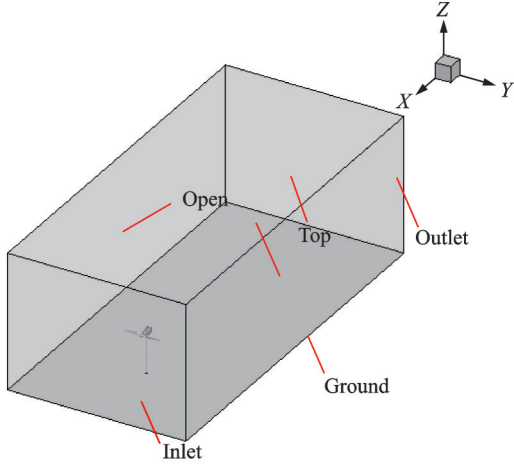


Fig.3 Computational domain and boundary conditions

defined function) is used to define the wind speed and the turbulent kinetic energy dissipation rate, according to the parameter change of experimental flow field, it is also used to determine the turbulent kinetic energy. No-slip wall is used to model the boundary layer of blade and the absolute rotation is determined, rotation domain is set to the MRF (Multi-reference frame), and the rotation speed is the same as the blade. Boundary condition of both slopes on the computation field is symmetric, and the pressure-outlet is used in the boundary layer outlet. In order to ensure the effect of the simulation, the velocity-inlet is employed on the boundary condition of the top on the field, and its direction is vertical to the inlet boundary layer inward. No-slip wall is used to model the boundary condition of ground, and the roughness height is computed according to Eq.(1). No-slip wall is also used in the remaining boundary layers

$$k_s = \frac{9.793z_0}{C_s} \quad (1)$$

where C_s is the roughness constant and in FLUENT default value is 0.5, surface roughness length in this wind tunnel experiment is 0.1^[19].

1.1.3 Mesh

The unstructured tetrahedral mesh is used to conduct the numerical computation here, and the blade surface, interface surface, static domain and rotation domain are encrypted to generate 2 165 664 nodes. The total number of grids is 11 975 796. The mesh of the blade and the area around the blade are encrypted, and the maximum size is 0.08 m for

blade and 0.3 m for the area around the blade. The size of the maximum mesh in all is 1.2 m, and the element quality of mesh metric is 0.848 17, which tends to 1.00, and meets the requirements of numerical investigation.

1.2 Wind shear model

For the SST $k-\omega$ turbulence model, Ijaz Fazil et al.^[19] proposed the logarithmic function of wind shear velocity as Eq.(2), the turbulent kinetic energy as Eq.(3), and SST $k-\omega$ turbulent dissipation rate as Eq.(4).

The wind shear is defined as

$$\bar{u}(z) = \frac{u_*}{K} \ln\left(\frac{z+z_0}{z_0}\right) \quad (2)$$

where z is the height above the ground, u_* the friction velocity, and z_0 the roughness length of the hilly terrain. $K = 0.4$ is the von-Karman constant.

The turbulence kinetic energy k is defined as

$$k = \frac{u_*^2}{\sqrt{C_\mu}} \quad (3)$$

where C_μ is the $k-\omega$ constant of turbulence model, and default value is 0.09 in FLUENT.

The $k-\omega$ turbulence dissipation rate ω is defined as

$$\omega = \frac{u_*^3}{K(z+z_0)} \quad (4)$$

1.3 Three-dimensional continuous hill model

The hilly terrain used here is obtained by rotating the Gaussian curve, Eq.(5), around the axis by 360°^[16]. The hill model is shown in Fig.4.

$$Z = h \times \exp\left(-0.5\left(\frac{X}{\sigma}\right)^2\right) \quad (5)$$

$$\sigma = \frac{L}{1.774}$$

where h is the height of hill and L the length measured in X direction between hill height from $h/2$ to h . The hill slope is defined as the average slope for the top half of the hill, $s = h/2L$. $h_1=15.8$ m is the height of the hill body 1, and $h_2=7.2$ m is the height of hill body 2, then $s_1 = 0.32$, $s_2 = 0.2$. According to Ref.[20], there is no flow separation behind the hills when the slope of hill is smaller than 0.3. The terrain 1 is composed of two hill bodies 1 and the terrain 2 is composed of the hill body 1 and

the hill body 2. The continuous model is shown in Fig.4.

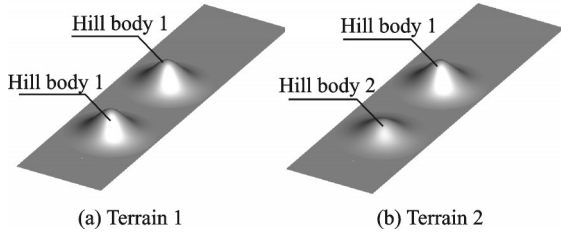


Fig.4 Three-dimensional continuous hill model

2 Results and Discussion

2.1 Calculation method verification

2.1.1 Wind turbine blade section pressure coefficient distribution

The pressure coefficients of the wind turbine blade at different stations, $r = 0.3R$, $0.47R$,

$0.63R$, $0.8R$, and $0.95R$, are predicted and compared with the experimental measurements shown in Fig.5.

It can be seen that the flow is attached in the most part of the blade surface, while airflow separation occurs on the leeward side of the blade. In addition, the predicted pressure coefficients at different sections are in good agreement with the experimental results. However, the pressure coefficient on the leeward side of the blade is slightly over-estimated. This is because SST $k-\omega$ turbulence model exists a little discrepancy when dealt with the flow separation problems. The airflow separation occurs at the leading edge of the blade, which is the most prominent at $0.95R$ shown in Fig.5 (f). Compared with the blade root, the wind speed of the blade root is higher and the stall zone is larger.

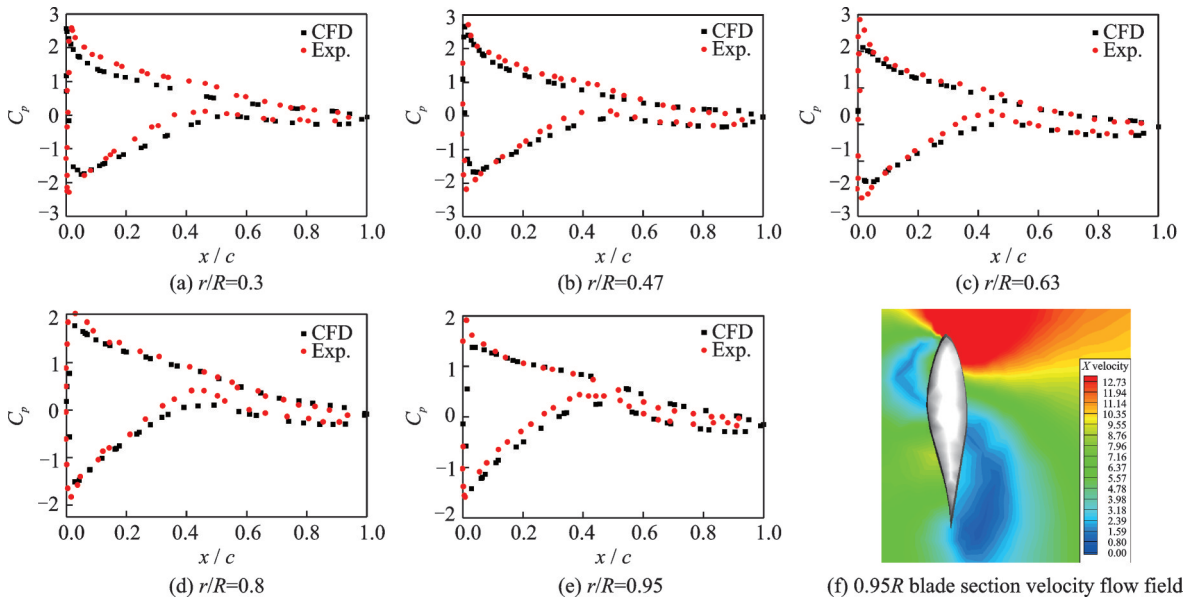


Fig.5 Sectional pressure coefficient of wind turbine blade under wind shear conditions

2.1.2 Wind speed distribution in wind turbine wake region

The wind speed from the aftward of wind turbines at different distances, $X = 2D$, $5D$, $10D$, $15D$, $20D$, is predicted and compared with the experimental measurements shown in Fig.6.

It is shown that the wake velocity distribution, at different locations in wind turbine wake regions, is in good agreement with the experimental results. However, there is a little discrepancy on

the wake velocity at the hub height. As the distance of X , wake direction, increases, the discrepancy gradually decreases. The main reason is that SST $k-\omega$ turbulence model has a certain discrepancy in accurately computing the rotation, and the stall zone occurs at high wind speed during the experiment. Even though there are some small discrepancies, the wake velocity distribution is predicted reasonably well.

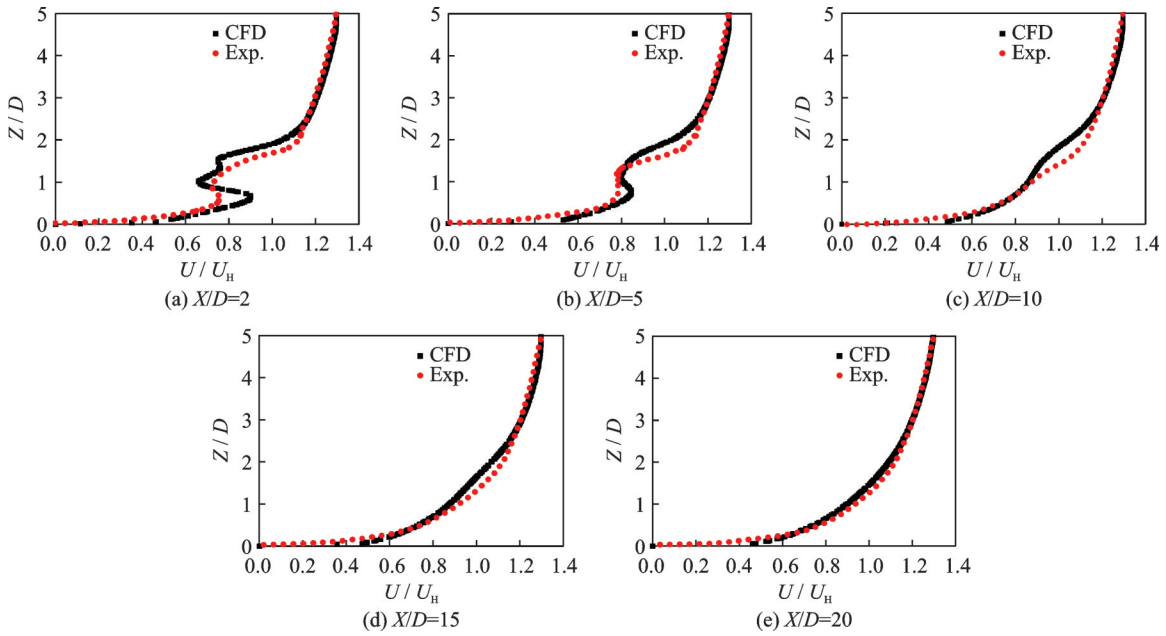


Fig.6 Wake velocity distribution at different locations under wind shear conditions

2.2 Influence of terrain 1 on the power of wind turbines

In terrain 1, a total of 9 aerodynamic numerical calculations are carried out. The 8th calculation position is located $1.5D$ on the left side of the center axis of the front hill body, and the 9th calculation position is located $1.5D$ on the left side of the central axis of the rear hill body, The position distribution of the previous 7 calculations is shown in Fig.7. The calculation results are shown in Table 1. The power ratio is the percentage of the power outputs of wind turbine in the hilly terrain to the power outputs of wind turbine in the flat terrain.

High-speed flow passes through the hilly terrain, the obvious stall effect in the flow field appears in the downhill, and the acceleration effect appears in the field on the top of hill, as shown in Fig.8. By comparing the results data of flat terrain and position 1 in Table 1, it is shown that the hills after the wind turbine has certain influence on the aerodynamic

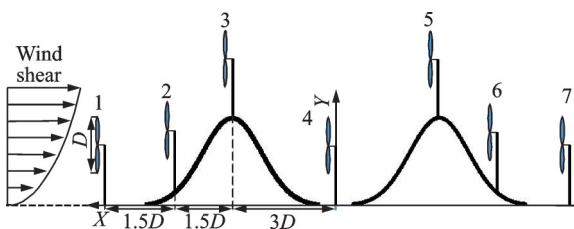


Fig.7 Distributions of wind turbine calculation position

Table 1 Power characteristics of wind turbines at different positions in terrain 1

Position	Thrust/kN	Torque/(N·m)	Power/W	Power ratio/%
Flat terrain	1 792.457	461.811	3 481.963	100.00
1	1 803.254	451.384	3 403.345	97.74
2	1 845.660	477.377	3 599.327	103.37
3	2 239.288	828.284	6 245.096	179.36
4	1 517.206	185.793	1 400.842	40.23
5	2 258.619	846.925	6 385.645	183.39
6	1 736.028	323.936	2 442.413	70.14
7	1 578.946	226.735	1 709.537	49.10
8	2 130.845	772.929	5 827.730	167.37
9	2 108.299	667.916	5 035.953	144.63

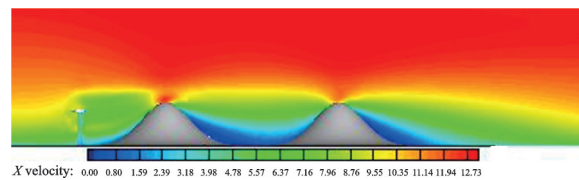


Fig.8 Flow field velocity distribution in terrain 1 position

characteristics. The power of the wind turbine in the position 1 is the lowest. As the distance between wind turbines and hills increases, the blockage effect caused by the hilly terrain is reduced and the ratio is close to 1. The wind turbine power of the position 2 is slightly larger than the position 1. The positions 4 and 7 are located in the stall zone, downstream of the hill terrain, but the power of the posi-

tion 4 are lower, and the stall zone, where the position 4 is located, is difficult to be recovered due to the influence of the rear hill. Comparing the positions 6 and 7, it can be found that the position 6 is located in the initial area of the stall zone, and the position 7 is located in the middle area of the stall zone, resulting in lower power compared with the position 7.

Comparing the positions 2 and 8, 6 and 9, it can clearly show that the power characteristics of the wind turbines located on the side of the hill are much larger than the position in the front and rear of the hill, the blockage effect appeared in front of and behind the wind turbine affects the power characteristics of the wind turbine seriously. Comparing the positions 3 and 5, the wind turbine power in the position 5 is higher due to the acceleration effect on the upper flow field caused by the top of hill, and the power output at position 8 is next.

2.3 Influence of terrain 2 on the power of wind turbines

In the terrain 2, the height of the front hill is reduced from 15.2 m to 7.2 m. A total of 9 aerodynamic simulation calculations are carried out, and the distribution of the calculation position is the same as above. The calculation results are shown in Table 2.

Table 2 Power characteristics of wind turbines at different locations in terrain 2

Position	Thrust/kN	Torque/(N·m)	Power/W	Power ratio/%
Flat terrain	1 792.457	461.811	3 481.963	100.00
1	1 806.337	455.004	3 430.639	98.53
2	1 840.352	581.800	4 386.656	125.98
3	2 122.709	679.031	5 119.758	147.04
4	1 712.047	378.648	2 854.930	81.99
5	2 255.401	758.085	5 715.809	164.15
6	1 761.271	348.908	2 630.697	75.55
7	1 620.645	260.325	1 962.798	56.37
8	1 990.702	593.180	4 472.459	128.45
9	2 109.323	671.090	5 059.884	145.32

It can be seen from Fig.9 that the front hill height is reduced. The stall zone in the downstream of the hill terrain is obviously reduced. Comparing

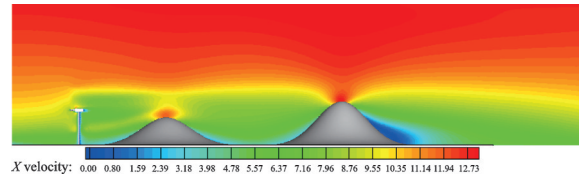


Fig.9 Flow field velocity distribution in terrain 2 position 1

the upstream positions 1 and 2, it is found that the wind turbine power characteristic of the position 2 is much larger than the position 1 because the position is raised and the incoming wind speed is increased. Comparing the positions 3 and 5, because the height of the position is increased, the wind turbine power characteristic of the position 5 is higher. The power characteristics of the positions 8, 9 are the same as the positions 3 and 5 because of different heights. In terrain 2, position 5 is still the best position in terms of power characteristics, and the power characteristics of the position 3 is next.

2.4 Influence of different terrains on the power of wind turbines

The height of the front hill is reduced, and the power output at the position 1 in the front hill is slightly increased, and the wind turbine is far from the hill body and the blockage effect caused by the hill is not obvious. However, the influence caused by the hill on position 2 is relatively large. When the thrusts of the wind turbine on different terrains are approximately equal, the power output in terrain 2 is much larger than that in terrain 1 because the blockage effect of the hill on the wake of the wind turbine is reduced. The position 3, due to the height influence, causes the incoming wind speed of the wind turbine in the terrain 2 to be reduced. At position 4, the height of the front mountain is reduced, the area of the stall area is reduced, and the incoming wind speed is recovered, the average thrust and power are greater than those of the wind turbine in the terrain 1.

In the rear hill, the flow field velocity in Figs.10(a) and (b) is compared. At terrain 1, the height of the front hill is reduced, and the acceleration effect caused by the hill top on the upper flow field is also weakened. Therefore, in the speed of the incoming flow absorbed by the wind turbine on

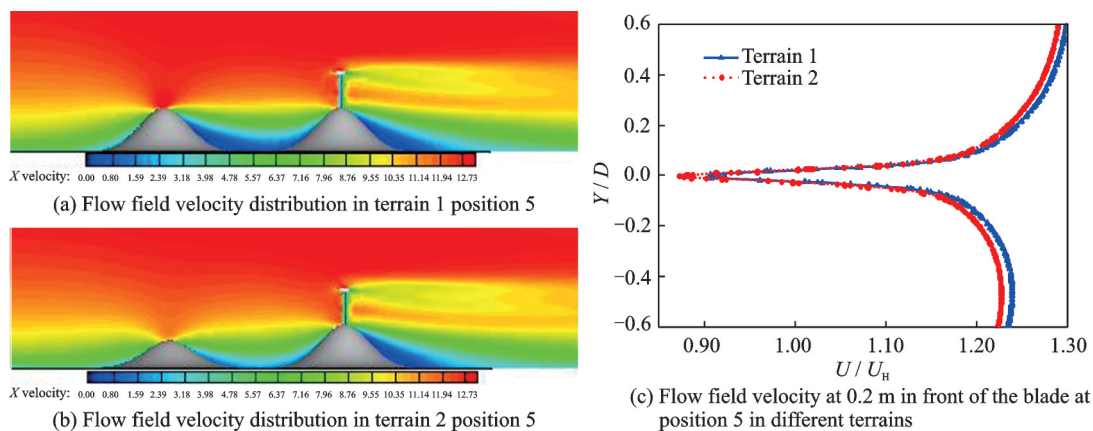


Fig.10 Comparison of flow field at position 5 in different terrains

the rear of the hill is reduced in terrain 2, as shown in Fig.10(c) and the power output is also reduced. For the positions 6, 7, due to the shrinkage of the stall zone, the power output of the position in the terrain 2 is strengthened. The position 8 in different terrains causes differences in power output because of the difference in height. At position 9, terrain 1 and terrain 2 have approximately the same power characteristics.

3 Conclusions

(1) A CFD-based approach, including a new aerodynamic model of three-dimensional hilly terrain and a wind shear model, is developed to investigate the complex aerodynamic interference between the two wind turbines and the hilly terrain. The proposed method is applied to the NREL Phase VI wind turbines and used to investigate the aerodynamic interaction between two wind turbines and hilly terrain. The pressure coefficients of the wind turbine blade at different stations agree well with the experiments over the atmospheric boundary layer, and the velocity distribution in the wake of the wind turbine is also predicted well, indicating the accuracy of the proposed method.

(2) In the same continuous hilly terrain, the top of the rear hill is the highest position for wind turbine power output, the left side of the front hill is next. The flow field on the top of the hill and the side of the hill has a higher wind energy density.

(3) When the height of the mountain is reduced, the area of the downstream stall zone is

slightly reduced, and the power output of the wind turbine located in the stall area and closed to the hill increases slightly, but the acceleration effect caused by the hill top on the upper flow field is also weakened, and the power characteristic of the wind turbines on the upper flow field is reduced.

The numerical analysis results play a reference role in adjusting the position of a single wind turbine in continuous hilly terrain. However, the proposed method for modeling continuous hilly terrain appears to be too simple, and further discussion is needed for the modeling of multiple actual mountain terrains. In addition, a single wind turbine is considered in the present work. Therefore, the aerodynamic characteristics of multiple wind turbines under complex hilly terrain conditions are further studied.

References

- [1] WEI T, OZBAY A, WEI Y, et al. An experimental study on the performances of wind turbines over complex terrain[J]. AIAA, Journal, 2013(3): 131-148.
- [2] OZBAY A, WEI T, YANG Z, et al. An experimental investigation on the wake interference of multiple wind turbines in atmospheric boundary layer winds[C]//AIAA Applied Aerodynamics Conference. [S.l.]: AIAA, 2006.
- [3] WEI Y, WEI T, OZBAY A, et al. An experimental study on the effects of relative rotation direction on the wake interferences among tandem wind turbines[J]. Science China Physics Mechanics & Astronomy, 2014, 57(5): 935-949.
- [4] SHAMSODDIN S, PORTÉ-AGEL F. Large-eddy simulation of atmospheric boundary-layer flow through a wind farm sited on topography[J]. Boundary-Layer

- Meteorology, 2016, 163(1): 1-17.
- [5] WEI T, OZBAY A, HUI H. An experimental investigation on the aeromechanics and wake interferences of wind turbines sited over complex terrain[J]. *Journal of Wind Engineering & Industrial Aerodynamics*, 2018, 172(2): 379-394.
- [6] KE Shitang, CAO Jiufa, WANG Long, et al. 3-D wind field simulation of wind turbine blades considering stationary wind correction and tower disturbance[J]. *Journal of Nanjing University of Aeronautics and Astronautics*, 2015, 47(1): 153-159.(in Chinese)
- [7] LU Chao, WANG Tongguang, XU Bofeng. Application of 3D dynamic stall model in aerodynamic characteristics calculation of wind turbines[J]. *Journal of Nanjing University of Aeronautics and Astronautics*, 2011, 43(5): 135-140.(in Chinese)
- [8] SHU Yan, SHI Shaoping, CHEN Xinming, et al. Numerical simulations of flow interactions between steep hill terrain and large scale wind turbine[J]. *Energy*, 2018, 151(2): 740-747.
- [9] SONG M X, CHEN K, HE Z Y, et al. Bionic optimization for micro-siting of wind farm on complex terrain[J]. *Renewable Energy*, 2013, 50(3): 551-557.
- [10] SONG M X, CHEN K, HE Z Y, et al. Optimization of wind farm micro-siting for complex terrain using greedy algorithm[J]. *Energy*, 2014, 67(4): 454-459.
- [11] SONG M X, CHEN K, HE Z Y, et al. Wake flow model of wind turbine using particle simulation[J]. *Renewable Energy*, 2012, 41(2): 185-190.
- [12] RICHARDS P J, NORRIS S E. Appropriate boundary conditions for computational wind engineering models revisited[J]. *Journal of Wind Engineering and Industrial Aerodynamics*, 2011, 99(4): 257-266.
- [13] IVANELL S, MIKKELSEN R, SRENSSEN J N, et al. Stability analysis of the tip vortices of a wind turbine[J]. *Wind Energy*, 2010, 13(8): 705-715.
- [14] IVANELL S, SRENSSEN J N, MIKKELSEN R, et al. Analysis of numerically generated wake structures[J]. *Wind Energy*, 2009, 12(1): 63-80.
- [15] PALMA J M L M, CASTRO F A, RIBEIRO L F, et al. Linear and nonlinear models in wind resource assessment and wind turbine micrositing in complex terrain[J]. *Journal of Wind Engineering and Industrial Aerodynamics*, 2008, 96(12): 2308-2326.
- [16] YANG Xiangsheng, ZHAO Ning, TIAN Linlin. Wake numerical simulation of wind field based on two modified wind engineering models[J]. *Transactions of Nanjing University of Aeronautics and Astronautics*, 2016, 33(1): 53-59.
- [17] MA Hongwang, CHEN Longzhu. Gravity effect on the first natural frequency of offshore wind turbine structures[J]. *Transactions of Nanjing University of Aeronautics and Astronautics*, 2016, 33(1): 95-101.
- [18] HAND M M, SIMMS D A, FINGERSH L J, et al. Unsteady aerodynamics experiment phase VI: Wind tunnel test configurations and available data campaigns [J]. *AIAA*, 2001, 562: 2303-2339.
- [19] Ijaz Fazil Syed Ahmed Kabir, NG E Y K. Effect of different atmospheric boundary layers on the wake characteristics of NREL phase VI wind turbine[J]. *Renewable Energy*, 2018, 130(5): 1185-1197.
- [20] MASON P J, KING J C. Measurements and predictions of flow and turbulence over an isolated hill of moderate slope[J]. *Quarterly Journal of the Royal Meteorological Society*, 2010, 111(468): 617-640.

Acknowledgements This work was supported by the Natural Science Foundation of Jiangsu Province (No. BK20161537), National Science Key Laboratory Foundation (No.6142220180202), Rotor Aerodynamics Key Laboratory Foundation (No.RAL20180303-1), and National Natural Science Foundation of China (No.11502105).

Authors Mr. ZHOU Tianyi is studying for a Master degree from Nanjing Tech University, and the research focuses on the influence between the complex terrain and the aerodynamic characteristics of wind turbines.

Dr. TAN Jianfeng received his B.S. degree in aircraft design from Nanjing University of Aeronautics and Astronautics (NUAA) in 2007, and the Ph.D. degree in aeronautical and astronautically science and technology from Tsinghua University, Beijing, China, in 2013, respectively. From 2017 to 2018, he was an Honor Associated Researcher in the CFD Laboratory, University of Glasgow, Scotland, UK. From 2013 to present, he has been with the School of Mechanical and Power Engineering, Nanjing Tech University, where he is currently a full associated professor. His research focuses on aerodynamics of rotor including rotorcraft and wind turbine, CFD, aeroacoustics, and

unsteady aerodynamic interaction.

Author contributions Mr. ZHOU Tianyi conducted the analysis, interpreted the results and wrote the manuscript.

Dr. TAN Jianfeng suggested the ideas for the study; Mr. CAI Jiangang, Mr. SHI Ruipeng, and Mr. XIA Yunsong jointly

performed all simulations under different conditions. All authors commented on the manuscript draft and approved the submission.

Competing interests The authors declare no competing interests.

(Production Editor: XU Chengting)

连续山丘地形上风力发电机功率输出特性数值分析

周天熠, 谭剑锋, 蔡建纲, 史瑞鹏, 夏云松

(南京工业大学机械与动力工程学院, 南京 211816, 中国)

摘要: 风力发电机在连续山丘上的位置对功率输出影响较大, 为研究双风机与山丘的复杂气动干扰, 建立了基于三维计算流体力学(Computational fluid dynamics, CFD)软件数值分析方法。该方法中, 建立新的三维丘陵模型以体现丘陵黏性效应, 通过对数函数构建风切变模型, 并嵌入“FLUENT”软件。随后将本方法应用于NREL Phase VI风力机, 并与大气边界层(Atmospheric boundary layer, ABL)风洞实验数据对比, 验证本文风力机气动特性分析方法的准确性。随后, 分析风力发电机在平坦地面和丘陵地形的风力机功率, 并改变风力机相对于丘陵位置以及第一个丘陵的形状。结果表明, 位于第二座山体顶部的风力机功率最高, 当风力机置于丘陵下游地区需尽量避免失速区, 且位于山体侧边风力机功率高于位于山体前后的风力机。

关键词: 功率特性; 风切变函数; NREL风力机; 连续丘陵地形; 仿真分析